Journal of Natural Pesticide Research 16 (2026) 100188

Contents lists available at ScienceDirect

Journal of Natural Pesticide Research

journal homepage: www.journals.elsevier.com/journal-of-natural-pesticide-research

Molecular network-based annotation of *Saccharomyces cerevisiae* and *Pachysolen tannophilus* metabolites and evaluation of their bioactive potential against rice pathogens *Magnaporthe oryzae*, *Bipolaris oryzae* and *Rhizoctonia solani*

Elizabeth G. Silva [a,*,1], Alana K. Pereira [b,2], Taicia P. Fill [c,3], Marta C.C. Filippi [d,4], Carlos A.G. Suarez [a,5], Inti D.C. Montaño [a,6], Vanessa G.P. Severino [a,*,7]

[a] Institute of Chemistry, Federal University of Goiás (UFG), Avenida Esperança, Campus Universitário, Goiânia GO, 74690-900, Brazil
[b] The Netherlands Organization for Applied Scientific Research (TNO), Sylviusweg 71, Leiden 2333 BE, the Netherlands
[c] State University of Campinas (UNICAMP), Laboratory of Microbial Chemical Biology (IQ-E-118), Institute of Chemistry – Department of Organic Chemistry, Cidade Universitária Zeferino Vaz, Barão Geraldo, Room E-119, Campinas, SP 13083-970, Brazil.
[d] Brazilian Agricultural Research Corporation (Embrapa) – Embrapa Rice and Beans, Rodovia GO-462, Km 12, Fazenda Capivara, Rural Zone, P.O. Box 179, Santo Antônio de Goiás, GO 75375-000, Brazil

ARTICLE INFO

Keywords:
Xylose
Dereplication
Diketopiperazines
Biocontrol
Rice fungal pathogens

ABSTRACT

This study investigates the biocontrol potential of extracts derived from the liquid co-cultivation of *Saccharomyces cerevisiae* and *Pachysolen tannophilus*, as well as from their respective monocultures, using xylose and xylulose as carbon sources, against phytopathogenic fungi affecting rice crops. LC-HRMS analysis, combined with advanced dereplication techniques, led to the annotation of several diketopiperazines, including cyclo(leucyl-prolyl), cyclo(phenylalanine-4-hydroxyproline), cyclo(prolylvalyl), cyclo(leucylvalyl), cyclo(phenyl-alanylprolyl), and cyclo(leucyl-4-hydroxyprolyl). The antifungal activity of the extracts was evaluated against *Magnaporthe oryzae*, *Bipolaris oryzae*, and *Rhizoctonia solani*, the causal agents of rice blast, brown spot, and sheath blight, respectively. *In vitro* assays included dual culture bioassays, assessments of conidial germination, and appressorium formation analysis. The co-culture extract completely inhibited appressorium formation (100%) and reduced conidial germination by 78%, exhibiting a minimum inhibitory concentration (MIC) of 1.25 mg/mL. Additionally, extracts from *P. tannophilus* at the same concentration showed notable antifungal effects, inhibiting 97.33% of appressorium formation and reducing conidial germination by 83.67% in *M. oryzae*, underscoring their potential in phytopathogen control. These findings indicate that the bioactive metabolites present in the extracts, particularly the annotated diketopiperazines, offer significant bioactive potential and represent a promising and sustainable alternative to conventional agrochemicals for rice disease management.

1. Introduction

In recent years, microorganisms—particularly fungi—have gained prominence as prolific sources of bioactive secondary metabolites with applications in medicine and agriculture. The characterization of these compounds relies on advanced analytical approaches, notably

* Corresponding author.
E-mail addresses: egs_beth@yahoo.com.br (E.G. Silva), alanakelyene@gmail.com (A.K. Pereira), taicia@gmail.com (T.P. Fill), cristina.filippi@embrapa.br (M.C.C. Filippi), carlogalen21@ufg.br (C.A.G. Suarez), inti@ufg.br (I.D.C. Montaño), vanessapasqualotto@ufg.br (V.G.P. Severino).
[1] https://orcid.org/0000-0002-2658-3756
[2] https://orcid.org/0000-0001-7190-9471
[3] https://orcid.org/0000-0003-4724-5251
[4] https://orcid.org/0000-0003-1676-8164
[5] https://orcid.org/0000-0002-6307-2031
[6] https://orcid.org/0000-0001-8509-0911
[7] https://orcid.org/0000-0001-5384-6657

https://doi.org/10.1016/j.napere.2026.100188
Received 13 November 2025; Received in revised form 14 March 2026; Accepted 24 March 2026
Available online 28 March 2026

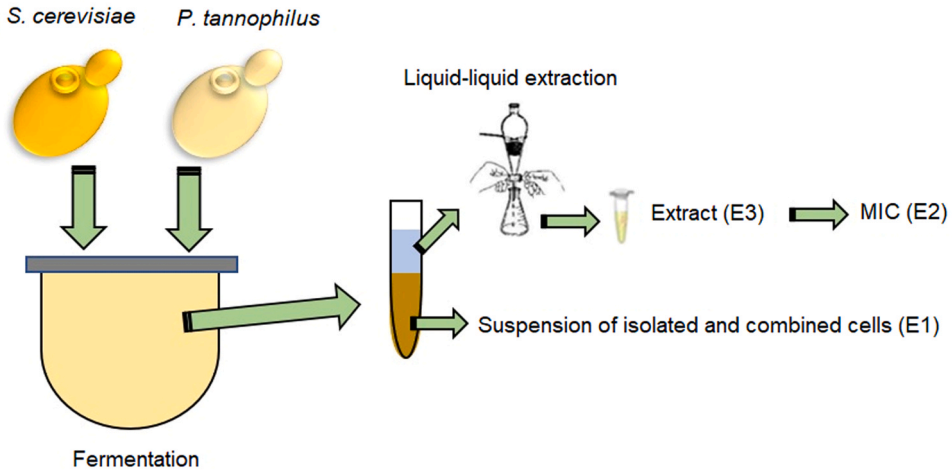

Fig. 1. – Summary of experiments: E1 – Efficiency of isolated and combined *S. cerevisiae* and *P. tannophilus* cell suspensions; E2 – Determination of the minimum inhibitory concentration (MIC) of the extract obtained from isolated cultures and co-culture of *S. cerevisiae* and *P. tannophilus*, solubilized in DMSO; E3 – Efficiency of the extract obtained from isolated cultures and co-culture of *S. cerevisiae* and *P. tannophilus*, solubilized in DMSO, in inhibiting conidial germination and appressorium formation of *M. oryzae* and *B. oryzae*.

spectrometric and spectroscopic techniques combined with bioinformatics tools and curated databases such as the Human Metabolome Database (HMDB), METLIN, *NUBBE DB*, *MassBank*, and the *Global Natural Products Social Molecular Networking platform* (*GNPS*) (Vieira et al., 2020). These integrated strategies have significantly enhanced the efficiency and reliability of natural product annotation.

Within this context, dereplication has emerged as a key strategy to accelerate metabolite annotation by enabling the early recognition of known compounds, thereby reducing redundancy and facilitating the discovery of novel bioactive molecules. Dereplication-based studies in fungal cultures have successfully identified metabolites with antiparasitic activity against *Trypanosoma brucei brucei (*Mazlan et al., 2020*)* and chemotherapeutic potential, as reported for *Cordyceps militaris* metabolites (Gao et al., 2020). Among fungal secondary metabolites, diketopiperazines (DKPs) have attracted particular attention due to their structural diversity and broad range of biological activities, including antimicrobial, antifungal, and antitumoral effects (Bushman et al., 2023). In agriculture, DKPs have shown promising potential as biocontrol agents, contributing to plant health and phytopathogen suppression while reducing dependence on synthetic pesticides (Rao et al., 2023).

Rice (*Oryza sativa* L.) is a staple food for more than half of the world's population, yet its production is severely affected by fungal diseases such as rice blast (*Magnaporthe oryzae*), grain spot (*Bipolaris oryzae*), and sheath blight (*Rhizoctonia solani*) (Tan et al., 2023). Rice blast is the most destructive of these diseases, capable of causing yield losses of up to 100% and threatening food security for millions of people (Hai-Feng et al., 2022). Grain spot ranks as the second most economically significant rice disease, particularly in endemic regions, (Prabhukarthikeyan et al., 2019) while sheath blight can reduce yields by 10–25%, reaching up to 50% under favorable conditions for pathogen development (Latif et al., 2022; Thuy et al., 2021).

Considering the global impact of these diseases and the urgent need for sustainable crop protection strategies, the investigation of fungal metabolites—especially DKPs—as biocontrol agents is both timely and relevant. Despite increasing interest in DKPs, studies addressing the co-cultivation of *Saccharomyces cerevisiae* and *Pachysolen tannophilus*, coupled with molecular networking to explore their metabolome in the context of rice disease management, remain scarce. Therefore, this study aims to characterize the chemical profile and evaluate the antifungal activity of metabolites produced during the co-cultivation of *S. cerevisiae* and *P. tannophilus* using a xylose–xylulose mixture as the carbon source. Metabolite annotation was performed by liquid chromatography coupled to high-resolution mass spectrometry (LC-HRMS), integrated with dereplication strategies and molecular networking, to identify compounds with potential biocontrol activity against major rice phytopathogens.

2. Materials and methods

2.1. Microbial strains and culture conditions

The microorganisms with antagonistic potential used in this study were the yeasts *S. cerevisiae*, obtained from the commercial brand Fleischmann®, and *P. tannophilus*, acquired from the André Tosello Foundation – Tropical Culture Collection. Both yeasts were cultured in a medium containing peptone (20 g/L), yeast extract (10 g/L), xylose (30 g/L), xylulose (10 g/L), and distilled water (YPX_1X_2 medium). The extracts used in this research were obtained from individual cultures as well as from a co-culture in which *S. cerevisiae* and *P. tannophilus* were combined at equal proportions (50% each), considering a liquid volume–to–well volume ratio of 47%. Fermentation was carried out in a shaking incubator at 30 °C and 130 rpm for 48 h, in triplicate, according to the protocols established by Silva et al. (2023), who identified these culture conditions as yielding the highest xylitol productivity.

The pathogenic microorganisms employed in this study included the fungi *M. oryzae*, *B. oryzae*, and *R. solani*, all obtained from the Microorganism Collection of EMBRAPA Rice and Beans.

2.2. Extraction of Metabolites from the Fermentation Medium

After fermentation, culture broths from both isolated and co-cultured strains were centrifuged at 9000 rpm for 15 min. The supernatants were extracted with ethyl acetate (1:1, v/v) in five sequential cycles. The resulting organic phases were pooled and concentrated using a rotary evaporator (Fisaton, model 801) at 200 rpm and 35 °C. The obtained extracts were reconstituted in methanol (2 mg/mL) for LC-HRMS analysis. An identical extraction procedure was applied to uninoculated $YPX_1{\times}_2$ medium, (Silva et al., 2023) serving as a control.

For biological activity evaluation, fermentation supernatants of both isolated and co-cultured yeasts were filtered after 48 h. Following supernatant removal, yeast cells were harvested for immediate use in antagonism assays. Extracts from fermentation media with higher xylitol production were dried, weighed, and reconstituted in 1 mL of dimethyl sulfoxide (DMSO) for testing.

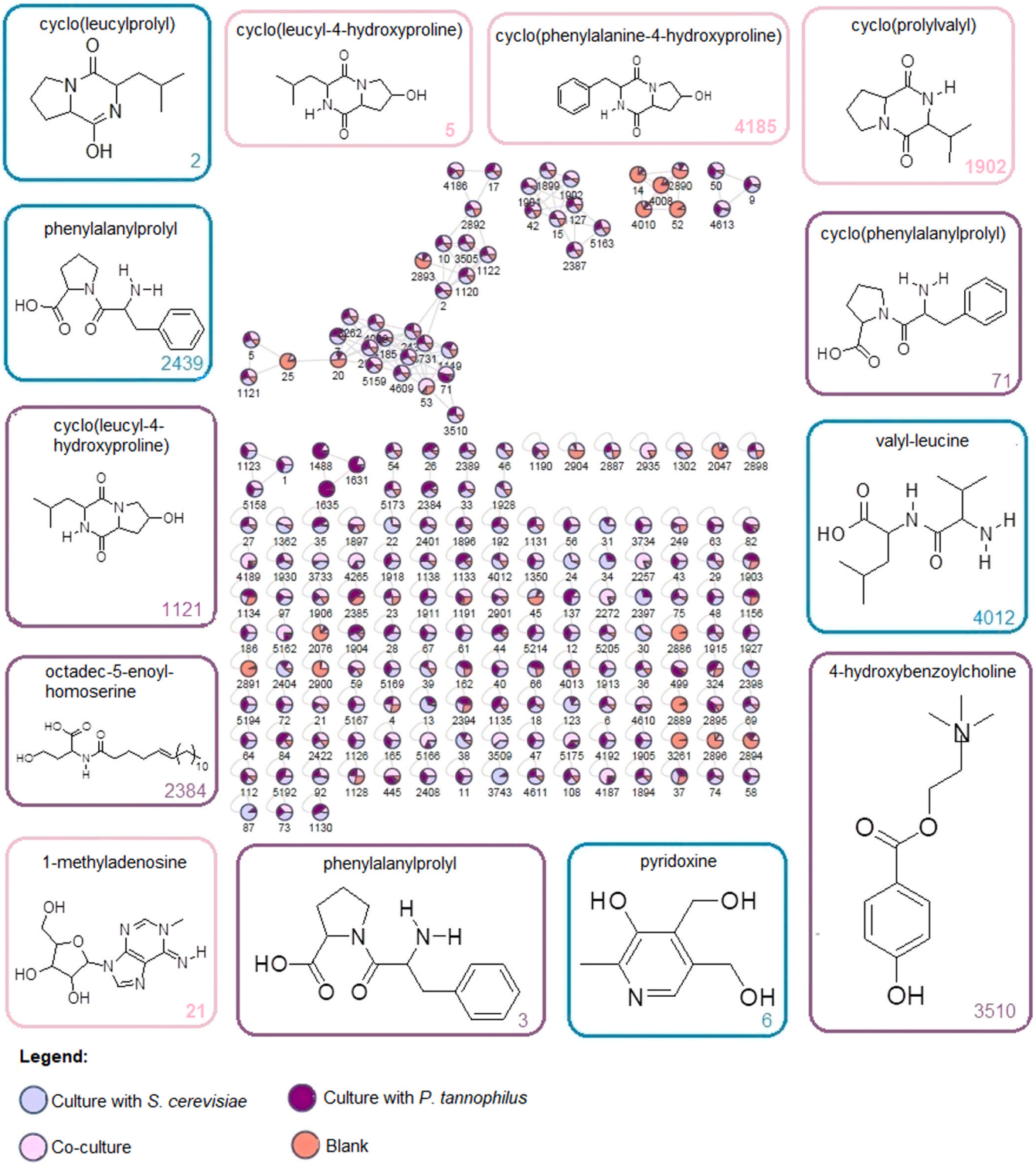

Fig. 2. – Molecular networks in FBMN mode, generated on the GNPS platform. Nodes are labeled by cluster ID.

2.3. LC-HRMS Analysis of the Extracts

Samples were analyzed by ultra-high performance liquid chromatography coupled with high-resolution tandem mass spectrometry (LC-HRMS). The system consisted of a Thermo Fisher RSLCnano U3000 UHPLC connected to a Thermo Scientific™ Q-Exactive mass spectrometer, equipped with a quadrupole-Orbitrap hybrid analyzer and a heated electrospray ionization (HESI) source.

Chromatographic separation was performed on an Accucore C_{18} column (5 µL injection volume), maintained at 40 °C, with a flow rate of 400 µL/min. The mobile phases were: (A) water with 0.1% formic acid, and (B) acetonitrile (ACN). The gradient was as follows: 5% B (0–5 min), 5–40% B (5–10 min), 40–45% B (10–12 min), 45–98% B (12–18 min).

The Q-Exactive Orbitrap was operated using Xcalibur 3.0 software under positive ionization mode with the following settings: spray voltage of + 3.5 kV (positive), capillary temperature 300 °C, S-lens RF

Table 1
Mass values (mg) of extracts obtained from monocultures of *S. cerevisiae* and *P. tannophilus*, and from co-culture, analyzed in triplicate.

Culture	Replicate 1 (mg)	Replicate 2 (mg)	Replicate 3 (mg)
S. cerevisiae	16.3	18.8	21.7
P. tannophilus	12.1	8.7	10.4
Co-culture	21.7	15.6	11.1

Annotated metabolites (GPNS library) are available at: https://gnps.ucsd.edu/ProteoSAFe/result.jsp?task=4c7a0dcdd8bd45759096c75144255864&view=view_all_annotations_DB. Noise filtering in MZmine 2 reduced GNPS annotations, underscoring the need for complementary tools (e.g., NAP, MASST) to interrogate unannotated features.

level 50 V, sheath gas flow 35 (arbitrary units), auxiliary gas 10 (arbitrary units), automatic gain control (AGC) target 1×10^6, maximum injection time (IT) 200 ms. Data were acquired at a resolution of 70,000 at *m/z* 200, in profile mode.

2.4. Feature-Based Molecular Networking (FBMN)

Spectral data (.mzML format) were processed using MZmine 2 (version 2.53) for noise removal and feature extraction (Pluskal et al., 2010). Processing steps included chromatogram building, deconvolution, isotope grouping, alignment, and gap-filling. Parameters were set as follows: noise level threshold 5.0E3, minimum retention time interval 0.01 min, *m/z* tolerance either 0.0 or 10.0 ppm. Peak alignment was performed using the Join Aligner algorithm, with *m/z* tolerance of 0.1 or 20 ppm. The resulting.csv and.mgf files were uploaded to the GNPS platform for FBMN analysis and MetaboAnalyst 5.0 for multivariate statistical analysis.

Molecular networks were visualized using Cytoscape (version 3.7.2). Principal Component Analysis (PCA) and Partial Least Squares Discriminant Analysis (PLS-DA) were conducted in MetaboAnalyst. Data were normalized and transformed to improve statistical robustness. Metabolites were evaluated based on Variable Importance in Projection (VIP) scores from the PLS-DA model. Cosine similarity scores close to 1 were considered indicative of high spectral similarity.

2.5. Antagonism Assays with Cultures and Extracts

Plates containing isolated phytopathogens in the absence of antagonistic yeasts, as well as those with pathogenic microorganisms grown on PDA medium (potato dextrose agar: 15 g/L agar, 200 g/L potato, 20 g/L dextrose), were used as controls. The pathogens were cultivated under different conditions. *M. oryzae* conidia were produced using a specific oatmeal-based medium (50 g/L oatmeal, 15 g/L agar, and 20 g/L dextrose), which was sterilized by autoclaving.

For assays, PDA plates containing the fungal pathogens were perforated using a sterile scalpel, and a 5 mm agar plug with mycelium was transferred to the center of a fresh PDA plate. Yeast suspensions or extracts were then applied according to the experimental design. Plates were incubated at 28 °C for 7 days, under light for *M. oryzae* and *R. solani*, and in the dark for *B. oryzae*.

Colony diameters were measured with a digital caliper. Mycelial growth inhibition was calculated using the method proposed by Hwang et al. (2022), comparing the treated and untreated colony areas. A summary of experiments E1, E2, and E3 is presented in Fig. 1.

2.6. Experiment E1 – Efficiency of isolated and combined S. cerevisiae and P. tannophilus cell suspensions

A completely randomized design (CRD) was used with four treatments: *S. cerevisiae* alone (E1.1), *P. tannophilus* alone (E1.2), co-culture (E1.3), and control (Figure A.30). Each treatment was replicated five times per phytopathogens, totaling 60 experimental units (plates). The culture pairing method was employed (Dennis and Webster, 1971). Cells used in the E1 assay were obtained from the evaluated culture medium after 48 h of fermentation. Following supernatant removal, the yeast biomass was employed in antagonism assays conducted in 90-mm Petri dishes. Phytopathogens were inoculated at the center of the plates, and 5 μL of the yeast cell suspension was subsequently applied. Inoculum distribution was standardized by delineating a 55-mm square, maintaining a 25-mm distance from the center. Plates were incubated at 28 °C for seven days, and antagonistic activity was assessed by measuring pathogen growth and calculating inhibition percentages.

2.7. Experiment E2 – Minimum Inhibitory Concentration (MIC) of Extracts from isolated cultures and co-culture of S. cerevisiae and P. tannophilus

The extracts obtained through liquid–liquid extraction and solubilized in DMSO were tested against *M. oryzae*, *B. oryzae*, and *R. solani*. The extracts were homogenized with 5 mL of sterile PDA medium in 15 mL centrifuge tubes and transferred to 60 mm Petri dishes. After solidification of the medium, a 5 mm plug of fungal mycelium was placed at the center of each plate. The concentrations of the extracts tested were 0.12, 0.25, 0.5, 0.75, 1.00, and 1.25 mg/mL.

To determine the MIC, a CRD was used with five treatments: extracts from *S. cerevisiae* alone (E2.1), *P. tannophilus* alone (E2.2), co-culture (E2.3), and controls (DMSO and water), with three replications for each phytopathogen studied (*M. oryzae*, *B. oryzae*, and *R. solani*). The most effective concentrations (0.75 mg/mL and 1.25 mg/mL) were used for detailed evaluation, totaling 270 experimental plates.

2.8. Experiment E3 – Inhibition of Conidial Germination and Appressorium Formation

Only *M. oryzae* and *B. oryzae* were used, as *R. solani* does not form appressoria. After 7 days of growth on PDA, mycelia were transferred to oat-agar medium and incubated for an additional 7 days. Aerial mycelium was scraped, and conidiogenesis was induced by incubating the plates for 48 h at 28 °C.

Conidia were collected with sterile water (2 mL), filtered, and used to prepare microscope slides. Humid chambers were assembled with sterile Petri dishes lined with moistened cotton and filter paper. Treatments: extracts from *S. cerevisiae* (E3.1), *P. tannophilus* (E3.2), co-culture of both yeasts (E3.3), and controls (DMSO and water). Conidial suspensions were mixed with extracts (at MIC) and placed on coverslips. Slides were incubated in humid chambers at 28 °C and observed every 2 h under an optical microscope (CX40RF200 – Olympus Optical, 10 × objective) for 12 h (Figure A.31).

2.9. Statistical Analysis

Statistical analysis was performed using Statistica 64 software. Significant differences in mycelial growth inhibition between treatments were determined using Tukey's test at $p < 0.05$.

Statistical analyses of the spectral data obtained from single cultures, co-culture, and the blank were performed using the MetaboAnalyst 5.0 platform, based on a table containing peak areas and their corresponding identifiers generated by MZmine 2 for molecular networking samples in FBMN mode. The data were imported as peak intensity matrices with samples arranged in columns and treated as unpaired. After data integrity verification, no interquartile range (IQR) variance filtering was applied; instead, data normalization was performed exclusively by scaling, using Pareto scaling for the classical analysis and autoscaling for the FBMN analysis. The CLUE-EM/EM dataset was subjected to multivariate analysis using unsupervised Principal Component Analysis (PCA), enabling the visualization of sample separation and the identification of variables responsible for this discrimination through loading plots. In addition, relevant metabolites were evaluated based on

Table 2
Metabolites derived from the extract obtained from the fermentation broth of the isolated culture using *S. cerevisiae*, annotated through FBMN analysis on the GNPS platform.

Node (ID)	Annotated Metabolite	Cosine Score (GNPS) / Score (NAP)	RT (min)	Exact Mass (*m/z*)	Observed Mass (*m/z*)	Error (ppm)	MS2	Chemical Structure	Molecular Formula
2*	cyclo(leucylprolyl)	0.89	4.38	210.1368	210.1365	-1.428	70, 86, 98, 83, 211	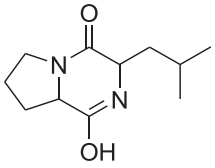	$C_{11}H_{18}N_2O_2$
7*	cyclo(phenylalanine-4-hydroxyproline)	0.78	4.00	260.1161	260.1158	-1.153	70, 91, 114, 185, 219, 260	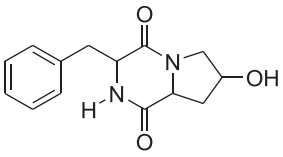	$C_{14}H_{16}N_2O_3$
1302*	cyclo(prolylvalyl)	0.79	1.71	196.1212	196.1210	-1.020	55, 70, 98, 141, 152, 169	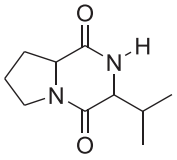	$C_{10}H_{16}N_2O_2$
6*	pyridoxine	1.00	1.00	169.0739	169.0738	-0.592	124, 134, 152, 154, 170	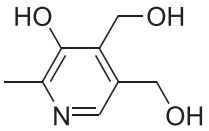	$C_8H_{11}NO_3$
2439**	phenylalanylprolyl	0.93	4.05	262.1317	262.1312	-1.907	70, 95, 125, 153, 245	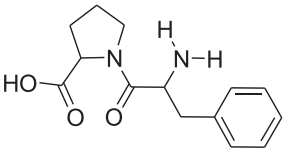	$C_{14}H_{18}N_2O_3$
3731**	cyclo (phenylalanylprolyl)	0.93	4.66	244.1212	244.1211	-0.410	71, 121, 153, 215, 246	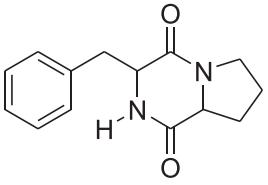	$C_{14}H_{16}N_2O_2$
4012**	valyl-leucine	0.92	4.84	230.1630	230.1627	-1.303	72, 86, 140, 168, 213	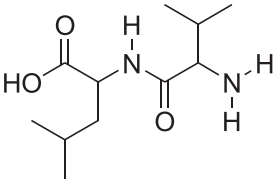	$C_{11}H_{22}N_2O_3$

*Selected by VIP scores through FBMN analysis on GNPS;
**Clusters containing only nodes belonging to this cultivation.
RT: retention time; N/A: not annotated.
NAP: Network annotation propagation.

Variable Importance in Projection (VIP) scores generated by Partial Least Squares Discriminant Analysis (PLS-DA), allowing the identification of the most influential variables contributing to group differentiation.

3. Results and discussion

3.1. Analysis of molecular networks

Using FBMN, 187 features were detected and grouped into clusters by index (ID) (Fig. 2), with each square labeled by its corresponding cluster ID. Among them, 19 features matched library spectra, predominantly diketopiperazines.

The extraction yields of all ethyl acetate extracts from each isolated strain and from the co-culture are presented in Table 1.

3.2. Selection of Relevant Metabolites

To prioritize the 187 detected features, multivariate analyses (PCA, PLS-DA) were performed. Features were annotated via high-resolution

Table 3
Metabolites derived from the extract obtained from the fermentation broth of the isolated culture using *P. tannophilus*, annotated by FBMN analysis on GNPS.

Node (ID)	Annotated Metabolite	Cosine Score (GNPS) / Score (NAP)	RT (min)	Exact Mass (*m/z*)	Observed Mass (*m/z*)	Error (ppm)	MS2	Chemical Structure	Molecular Formula
2384**	octadec-5-enoyl-homoserine	0.89	3.51	383.3036	383.3035	-0.261	57, 70, 98, 120,345	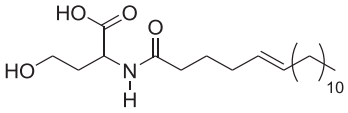	$C_{22}H_{41}O_4N$
3**	phenylalanylprolyl	0.93	4.66	262.1317	262.1313	-1.526	70, 98, 120, 153, 245	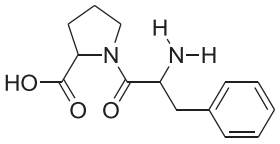	$C_{14}H_{18}N_2O_3$
1121**	cyclo(leucyl-4-hydroxyprolyl)	0.78	3.63	226.1317	226.1315	-0.884	86, 200, 226, 228	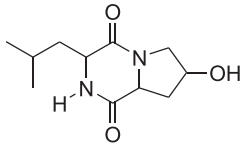	$C_{11}H_{18}N_2O_3$
2888**	cyclo(phenylalanyl-4-hydroxyprolyl)	0.79	3.94	260.1161	260.1160	-0.384	70, 91, 114, 185, 213, 259	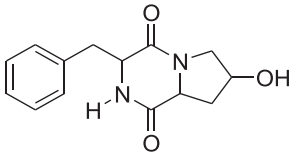	$C_{14}H_{16}N_2O_3$

*Selected by VIP scores through FBMN analysis on GNPS;
** Clusters containing only nodes belonging to this culture.
RT: retention time; N/A: not annotated.
NAP: Network annotation propagation.

MS/MS spectra on GNPS and validated against literature and public databases (PubChem, SciFindern).

3.3. Metabolites Annotated by FBMN Analysis

Results revealed cyclic peptides (diketopiperazines). Annotated compounds included cyclo(leucylprolyl), cyclo(phenylalanine-4-hydroxyproline), cyclo(prolylvalyl), cyclo(leucylvalyl), cyclo(phenylalanylprolyl), and cyclo(leucyl-4-hydroxyproline) (clusters shown in Figure A.32a, highlighted by the VIP scores analysis in FBMN mode.

The precursor ion *m/z* 197.1282 (cluster 3505) was annotated as cyclo(prolylvalyl) with cosine similarity 0.97. High spectral match (cosine 0.97) confirmed cyclo(prolylvalyl) (Fig. A.32b).

Cyclo(prolylvalyl) is reported for antibacterial activity against MRSA (Zin et al., 2020) and antifungal action against *Fusarium graminearum* (Jamal et al., 2017). The minimum inhibitory concentration (MIC) required to inhibit the visible mycelial growth of *F. graminearum* was 250 μg/mL, while 1000 ppm were sufficient to completely inhibit its growth on wheat grains after 10 days of incubation.

Additionally, cyclo(prolylvalyl) limits *F. oxysporum f. sp. lycopersici* conidial germination and alters hyphal morphology; *in vivo* conditions, this compound suppresses *Fusarium* wilt and promotes tomato growth (Hwang et al., 2022).

The precursor ion *m/z* 245.1285 (cluster 3731) matched cyclo(phenylalanylprolyl) (cosine 0.93) (Figure A.32a). The cyclic dipeptides cyclo(leucylprolyl) and cyclo(phenylalanylprolyl) exhibited broad antimicrobial activity, inhibiting the growth of lactic acid bacteria (*Lactobacillus casei* AST18, *L. plantarum* MiLAB 393, *L. plantarum* LBP-K 10, *L. reuteri* RC-14, and *L. lactis*) as well as the opportunistic yeast *Candida albicans* (Zheng et al., 2022).

Cyclo(phenylalanylprolyl) exhibited an MIC of 8 μg/mL against *Aspergillus flavus* MTCC 277, significantly suppressing both mycelial growth and aflatoxin biosynthesis - properties that underscore its potential as a natural biopreservative for controlling fungal contamination and mycotoxin formation in food and feed (Kumar et al., 2013).

The precursor ion *m/z* 211.1439 (cluster 2) was annotated as cyclo(leucylprolyl) (cosine 0.89). Spectral comparison confirmed this compound, which inhibits aflatoxin production by *Aspergillus parasiticus* and shows MIC of 12.5 μg/mL (*Mucor ramannianus*), 5.0 μg/mL (*Rhizoctonia solani*), and 2.5 μg/mL (*Pyricularia oryzae*), reinforcing its potential as antifungal agent (Sibanda et al., 2017).

Moreover, antagonistic yeasts tend to accumulate elevated levels of diketopiperazines – particularly cyclo(leucylprolyl) and cyclo(phenylalanylprolyl) – which contribute to their antifungal efficacy (Maluleke et al., 2022). Similarly, cyclic dipeptides such as cyclo(gly-pro), cyclo(ala-leu) and cyclo(leucylprolyl) isolated from *Bacillus vallismortis* effectively suppressed phytopathogens (including *Pseudomonas syringae* in *Arabidopsis*), further validating their role in crop protection (Noh et al., 2017). FBMN analysis of samples consistently highlighted diketopiperazine as the dominant bioactive subclass.

Given the expanding characterization of cyclic dipeptides with relevant biological activities, as observed in fungi, (Wang et al., 2017) continued investigation into their properties and applications is strongly warranted.

The compounds identified via GNPS, along with their LC–MS/MS chromatograms, are presented in Tables 2, 3, and 4.

3.4. Experiment E1 - Efficiency of isolated and combined S. cerevisiae and P. tannophilus cell suspensions

Experiment E1 was conducted to evaluate the *in vitro* antagonistic activity of isolated and combined cell suspensions of *S. cerevisiae* and *P. tannophilus* against three major rice pathogens (*M. oryzae*, *B. oryzae* and *R. solani*). In the *M. oryzae* assays, the control plates reached 7.33

Table 4
Metabolites derived from the extract obtained from the fermentation broth of the coculture using *S. cerevisiae* and *P. tannophilus*, annotated by FBMN analysis on GNPS.

Node (ID)	Annotated Metabolite	Cosine Score (GNPS) / Score (NAP)	RT (min)	Exact Mass (*m/z*)	Observed Mass (*m/z*)	Error (ppm)	MS2	Chemical Structure	Molecular Formula
5*	cyclo(leucyl-4-hydroxyprolyl)	0.78	3.63	226.1317	226.1316	-0.884	86, 200, 226, 228	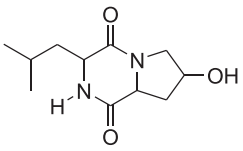	$C_{11}H_{18}N_2O_3$
53**	phenylalanylprolyl	0.94	1.63	262.1317	262.1315	-0.763	70, 95, 125, 153, 245	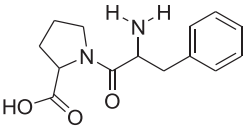	$C_{14}H_{18}N_2O_3$
4185**	cyclo(phenylalanyl-4-hydroxyprolyl)	0.79	4.00	260.1161	260.1160	-0.384	70, 91, 114, 185, 219, 260	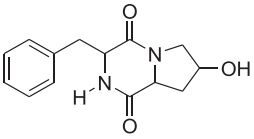	$C_{14}H_{16}N_2O_3$
4186**	cyclo(prolylvalyl)	0.82	1.19	196.1212	196.1211	-0.510	55, 70, 98, 141, 152, 169	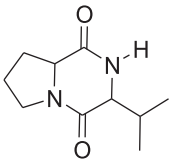	$C_{10}H_{16}N_2O_2$
21**	1-methyladenosine	0.98	1.00	281.1124	281.1116	-2.846	149, 278, 281	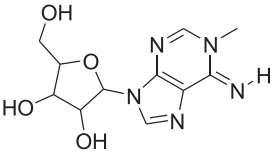	$C_{11}H_{15}N_5O_4$

*selected by VIP score in the GNPS FBMN analysis;
** clusters containing only nodes belonging to this culture.
RT: retention time; N/A: not annotated.
NAP: Network Annotation Propagation.

± 0.56 cm, while treatments with *S. cerevisiae* (E1.1), *P. tannophilus* (E1.2) and their co-culture (E1.3) yielded diameters of 4.38 ± 0.47 cm (62.99% inhibition), 5.17 ± 0.45 cm (50.21% inhibition) and 4.85 ± 0.27 cm (56.28% inhibition), respectively.

Against *B. oryzae*, control colonies measured 5.28 ± 0.14 cm; in E1.1 they measured 3.22 ± 0.15 cm (80.79% inhibition), in E1.2 3.78 ± 0.09 cm (73.52% inhibition) and in E1.3 3.70 ± 0.12 cm (73.28% inhibition), with observations revealing hyphal thinning and distortion indicative of cell-wall disruption by yeast metabolites. For *R. solani*, the control averaged 8.29 ± 0.00 cm, whereas E1.1 measured 5.43 ± 0.31 cm (34.52% inhibition), E1.2 3.51 ± 0.22 cm (57.65% inhibition) and E1.3 1.37 ± 0.18 cm (83.51% inhibition). Overall, both individual and combined yeast treatments significantly reduced mycelial growth of all three pathogens, with the co-culture (E1.3) consistently producing the highest inhibition rates (Fig. 3a–c).

3.5. Experiment E2: Determination of the Minimum Inhibitory Concentration (MIC) of extracts obtained from isolated cultures and co-cultures of S. cerevisiae and P. tannophilus against the pathogens M. oryzae, B. oryzae, and R. solani

The main objective of Experiment E2 was to determine the minimum inhibitory concentration (MIC) of concentrated extracts (E2.1, E2.2 and E2.3) against *M. oryzae*, *B. oryzae* and *R. solani in vitro*. Initial assays at 0.12, 0.25 and 0.5 mg/mL proved ineffective; subsequent tests were conducted using concentrations of 0.75 and 1.25 mg/mL. In assay E2.1, the concentration of 0.75 mg/mL resulted in an inhibition of 33.40%, and 1.25 mg/mL increased the inhibition to 68.77%. In assay E2.2, inhibitions were 22.06% and 40.10% at the respective concentrations, highlighting significant differences in relation to the control-DMSO. At E2.3, inhibition increased to 37.94% and 60.40% for the same concentrations, also with significant differences compared to control-DMSO. Statistical analysis using the Tukey test ($p < 0.05$) confirmed the effectiveness of the higher concentrations, showing that the concentration of 1.25 mg/mL was more effective in reducing mycelial growth, attesting to the fungistatic potential of the metabolites in the extracts, especially with *P. tannophilus* and co-cultivation (Fig. 4a).

In the E2 assay carried out to evaluate the antagonistic activity of yeasts against *B. oryzae*, a fungistatic effect of the concentrated extracts on the mycelial growth of the fungus was observed. The minimum inhibitory concentration (MIC) was evaluated, confirming a reduction in pathogen growth, with inhibitions of 60.19% and 76.40% at concentrations of 0.75 mg/mL and 1.25 mg/mL, respectively. Tukey's statistical test revealed that only treatments with extracts of E2.1 (1.25 mg/mL) and E2.2 (0.75 mg/mL) did not show a significant difference in relation to the DMSO control. The results indicate that the secondary metabolites of the extracts have antifungal potential, suggesting interactions with the fungal cell wall that inhibit enzymes involved in mycelial growth (Fig. 4b).

In assays against *R. solani*, 0.75 mg/mL inhibited mycelial growth by 54.76%, 23.40% and 18.70% in experiments E2.1, E2.2 and E2.3, respectively, while 1.25 mg/mL achieved 98.41% (E2.1), 83.75% (E2.2) and 83.49% (E2.3) inhibition. All treatments showed statistically

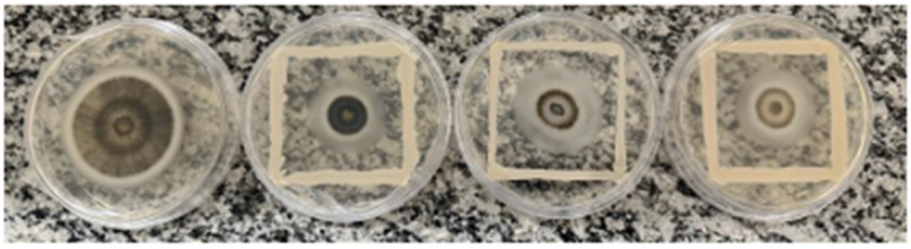

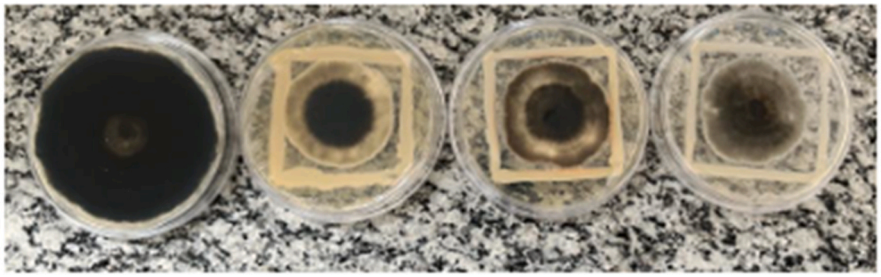

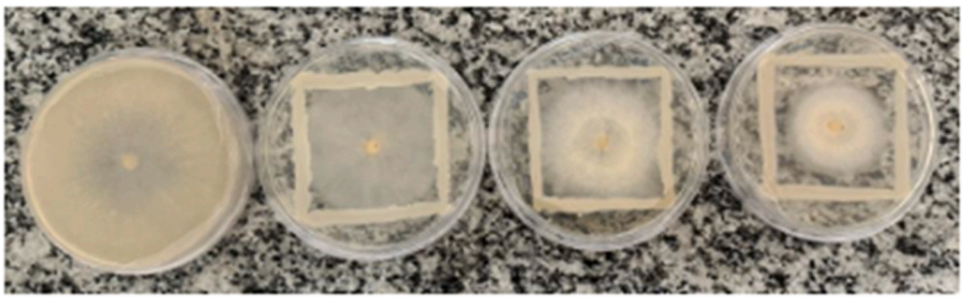

Fig. 3. – *In vitro* antagonistic efficacy of isolated and combined cell suspensions of *S. cerevisiae* and *P. tannophilus* against (a) *M. oryzae*, (b) *B. oryzae* and (c) *R. solani*. Control: pathogen alone on PDA medium. *P. tannophilus* treatment: pathogen paired with *P. tannophilus*; *S. cerevisiae* treatment: pathogen paired with *S. cerevisiae*; co-culture: pathogen paired with simultaneously with both *S. cerevisiae* and *P. tannophilus*.

significant reductions compared to the DMSO control ($p < 0.05$) (Fig. 4c).

Studies using the culture filtrate of *Streptomyces sp*. grown in a medium containing glucose, malt extract, and peptone, with 100 µL of the filtrate applied per well on PDA plates (potato extract, dextrose, and agar), resulted in a 69.00% inhibition of *R. solani* mycelial growth (Tamreihao et al., 2016).

These findings reinforce the potential of the extracts evaluated in this study as effective alternatives for the control of *R. solani*, with inhibition levels reaching up to 83.75%.

3.6. Experiment E3 – Inhibition of Conidial Germination and Appressorium Formation

In vitro assays (E3) were conducted to evaluate the effects of yeast-derived extracts on conidial germination and appressorium formation against *M. oryzae* and *B. oryzae*. Conidial suspensions were incubated in three treatments — E3.1 (*S. cerevisiae* extract), E3.2 (*P. tannophilus* extract), and E3.3 (co-culture extract of *S. cerevisiae* + *P. tannophilus*) — alongside water and DMSO (negative controls). All treatments were applied at a final concentration of 1.25 mg/mL.

Regarding *M. oryzae,* after 4 h of incubation, 10.34% of conidia in the water control had developed germ tubes. In contrast, germ-tube emergence and appressorium formation were completely inhibited by the DMSO control and all extract treatments at this time point. Notably, treatment E3.1 achieved complete (100%) inhibition of appressorium formation and reduced conidial germination to 33.33% after 12 h. Furthermore, E3.1 significantly delayed the onset of germination: only 6.25% of conidia germinated at 6 h, compared to 52.63% in the water control and 15.00% in the DMSO control. After 12 h, germination in the controls increased to 80.00% (water) and 45.54% (DMSO), while treated conidia remained devoid of appressoria (Fig. 5a). These findings highlight the importance of appressorium inhibition in preventing *M. oryzae* infection and reinforce the potential of the tested extracts as effective antifungal agents.

Treatment E3.2 markedly reduced conidial germination and appressorium formation: after 10 h, only 2.45% of conidia had germinated and 2.28% had developed appressoria. In contrast, the water control exhibited 95.92% germination and 67.11% appressorium formation, while the DMSO control showed 90.11% and 76.78%,

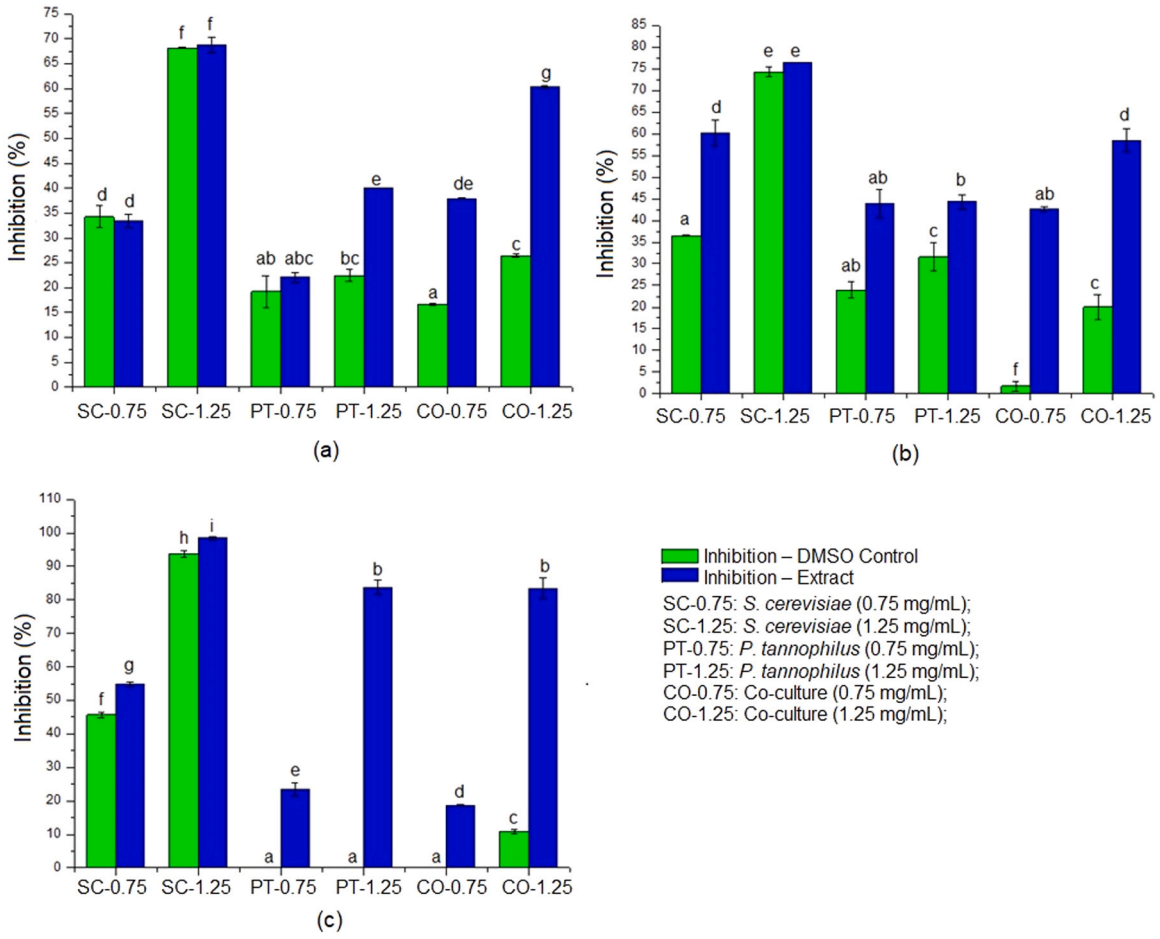

Fig. 4. – Growth inhibition (%) of (a) *M. oryzae*, (b) *B. oryzae*, and (c) *R. solani* on control plates (DMSO) and plates treated with concentrated diketopiperazine extracts obtained from the fermentations of *S. cerevisiae* and *P. tannophilus*, at concentrations of 0.75 mg/mL and 1.25 mg/mL for MIC determination. Control-DMSO: pathogen colony grown on PDA medium in the presence of DMSO. Treatment with *P. tannophilus*: pathogen colony grown on PDA medium with extract from the isolated *P. tannophilus* culture. Treatment with *S. cerevisiae*: pathogen colony grown on PDA medium with extract from the isolated *S. cerevisiae* culture. Co-culture treatment: pathogen colony grown on PDA medium with extract from the co-culture of *S. cerevisiae* and *P. tannophilus*. Means followed by the same letters do not differ significantly from each other according to Tukey's test ($p < 0.05$).

respectively. At 12 h, germination and appressorium formation in the water control reached 100% germination and 85%, respectively, whereas in the treated group, they remained at 16.33% and 2.67% — corresponding to 83.67% and 97.33% inhibition relative to water control (Fig. 5b). Treatment E3.3 showed the strongest antifungal activity. After 6 h of incubation, conidial germination was limited to 11.77%, compared to 84.85% in water control. By 12 h, the treatment inhibited conidial germination by 85.71% of germination and 97.96% of appressorium formation (Fig. 5c).

The mature appressorium is essential to the infection cycle of *M. oryzae*, as it generates sufficient turgor pressure to mechanically breach the host cuticle and cell wall. After penetration, primary invasive hyphae develop and subsequently differentiate into secondary infectious hyphae that colonize adjacent host cells. New conidia are produced by aerial conidiophores 3–5 days post-infection, thereby completing the disease cycle (Xiao et al., 2023).

GNPS - based annotation afforded several diketopiperazines - including cyclo(leucylprolyl), cyclo(phenylalanine-4-hydroxyproline), cyclo(prolylvalyl), cyclo(leucylvalyl), cyclo(phenylalanylprolyl) and cyclo(leucyl-4-hydroxyproline) — which are likely responsible for the observed antifungal activity. All extract treatments inhibited appressorium formation between 97.00% and 100.00%, undercoring the potential of diketopiperazines as promising agents against rice blast disease.

Studies with the crude extract of *Epicoccum sp.* demonstrated significant efficacy in controlling *Magnaporthe oryzae*, the causal agent of rice leaf blast. In in vitro assays, when applied the extract at a concentration of 0.6 mg/mL, the extract inhibited 95.68% of appressorium formation, (Sena et al., 2013) aligning with the present findings for *P. tannophilus* and co-culture extracts, and with the *S. cerevisiae* extract achieved complete (100%) inhibition of appressorium formation.

The results of the experiments involving *B. oryzae* are presented in the following order. Initially, all treatments exhibited inactive conidia. After two hours, it was observed that 58.21% of the conidia germinated in the water control, while only 18.07% germinated in the DMSO control. In contrast, the treatment with the extract (E3.3) resulted in complete inhibition of germination. As the experiment progressed, germination in the water control reached 100% after 10 h, compared to 44.95% in the DMSO control and 23.47% in the E3.3. Notably, the extract also completely prevented the formation of appressoria. After 12 h, E3.3 maintained a 71.43% inhibition of conidial germination and 100% inhibition of appressorium formation, demonstrating its potential as a promising fungistatic agent against *B. oryzae* (Fig. 6).

Experiments E3.1 and E3.2 showed lower inhibitory effects compared to experiment E3.3. In experiment E3.1, germination also started after 6 h, reaching 42.53%, compared to 51.32% in the water control. After 10 h, the water control showed 69.36% germination and 69.41% appressorium formation. At 12 h, germination and appressorium formation in the water control reached 93.75% and 76.04%,

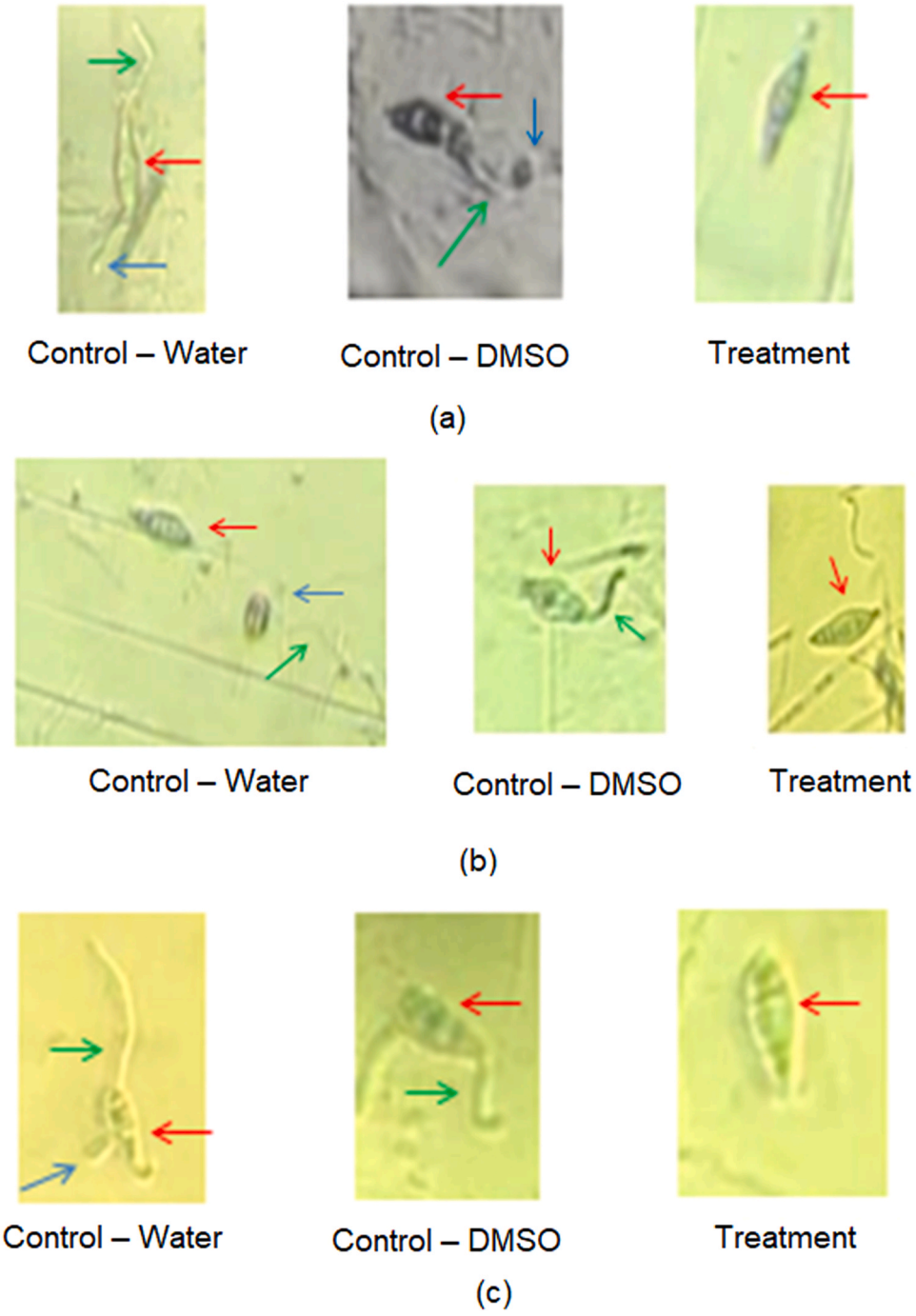

Fig. 5. – Effectiveness of the 1.25 mg·mL^{-1} extract treatments in inhibiting *M. oryzae* conidial germination and appressorium formation after 12 h. (a) *S. cerevisiae* extract; (b) *P. tannophilus* extract; (c) co-culture extract. Water control: conidia suspended in sterile water; DMSO control: conidia in 1% DMSO. (Red arrow: conidium; green arrow: germ tube; blue arrow: appressorium.).

respectively, while E3.1 resulted in 75.16% germination and 14.91% appressoria (Fig. 7a). In experiment E3.2, after 12 h, all conidia had germinated and formed appressoria, as shown in Fig. 7b. Germination began after 6 h, reaching 12.66%, with 5.06% of the conidia forming appressoria. After 8 h, germination increased to 55.56%, and by 10 h, 35.71% of conidia had germinated, with 28.57% forming appressoria. Although no significant inhibition of germination was observed in experiments E3.1 and E3.2, the results suggest that metabolites from the diketopiperazine class may have positively influenced fungal development compared to the DMSO control.

Studies using *B. oryzae* isolates cultivated on Petri dishes containing PDA medium (potato dextrose agar), supplemented with 50 µL of *Bacillus sp*. and *Serratia marcescens* extracts solubilized in 1 mL of dimethyl sulfoxide (DMSO), showed a 37.8% reduction in *B.* oryzae mycelial growth with *Bacillus sp*. extracts (after 16 h incubation), while *S. marcescens* extracts resulted in a 17.2% reduction under the same conditions (Elias et al., 2023). Other studies reported inhibition rates of approximately 93% against *B. oryzae* under in vitro conditions, using the crude extract method with *Trichoderma* strains at 10 g/L incorporated into potato-dextrose-agar medium (Klaram et al., 2022).

The yeast–pathogen interactions in this study exhibited a more pronounced fungistatic effect with *S. cerevisiae* cells compared to the co-

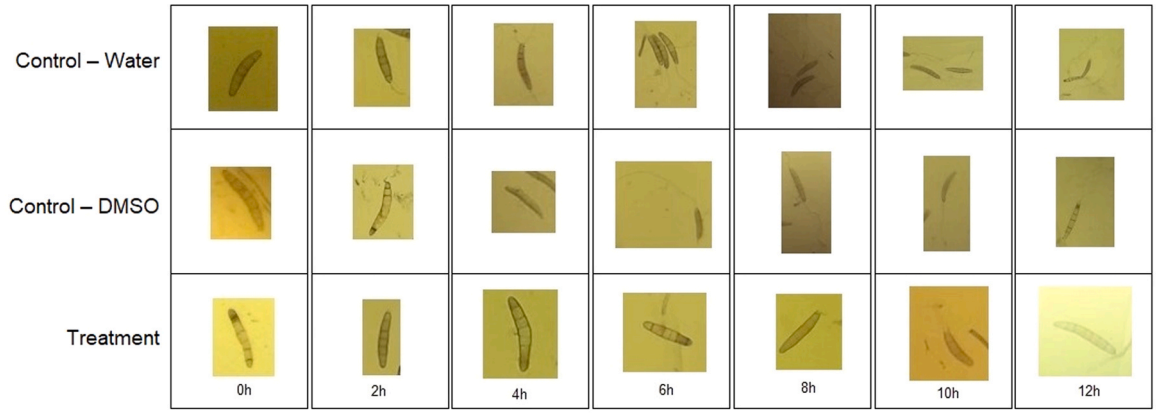

Fig. 6. – Inhibitory effect of the extract obtained from the *S. cerevisiae* and *P. tannophilus* co-culture (E3.3) (1.25 mg/mL) on conidial germination and appressorium formation of *B. oryzae* after 12 h of incubation. Treatments: Water control (conidia incubated in distilled water); DMSO control (conidia incubated in 1% DMSO); Co-culture treatment (conidia incubated in the co-culture extract). Arrows: red – conidium; green – germ tube; blue – appressorium.

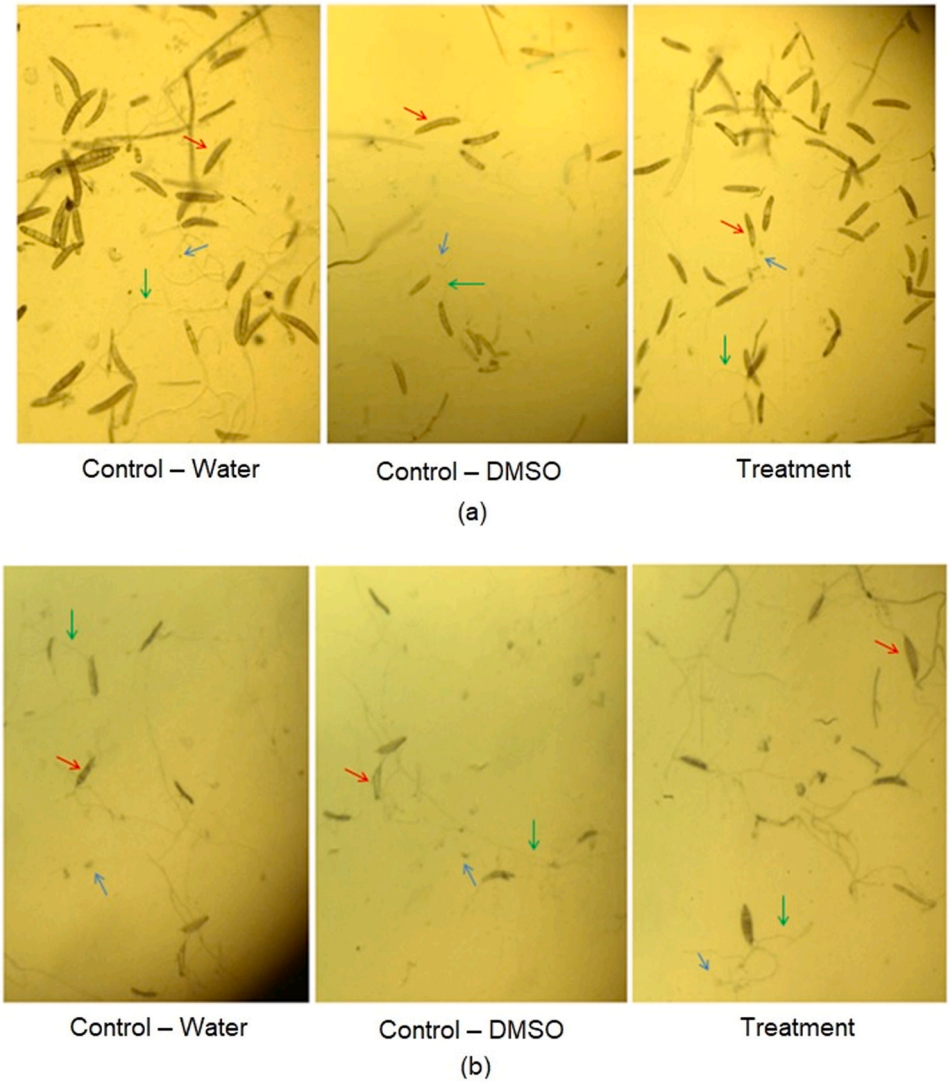

Fig. 7. – Inhibitory effect of the extract obtained from isolated yeast cultures (1.25 mg/mL) on conidial germination and appressorium formation of *B. oryzae* after 12 h of incubation. (a) *S. cerevisiae* extract treatment (E3.1); (b) *P. tannophilus* extract treatment (E3.2); Controls: Water control (conidia in distilled water); DMSO control (conidia in 1% DMSO). Arrows: red – conidium; green – germ tube; blue – appressorium.

culture. Although supernatants from isolated fermentations of *S. cerevisiae* and *P. tannophilus* did not show direct antifungal activity,

they caused morphological alterations in *M. oryzae*, *B. oryzae*, and *R. solani*. The most effective MIC of the concentrated diketopiperazine extracts was 1.25 mg/mL.

Statistical analyses demonstrated that extracts from isolated *P. tannophilus* and the co-culture significantly inhibited fungal development compared to the DMSO control and were more effective than *S. cerevisiae* alone against all three pathogens evaluated. Analysis of conidial germination and appressorium formation showed an average suppression of 98% in appressorium formation and approximately 80% inhibition of conidial germination of *M. oryzae*. For *B. oryzae*, co-culture extracts inhibited 100% of appressorium formation and reduced germination by 71%.

This study pioneers the investigation of antifungal activity of concentrated diketopiperazine extracts, highlighting their potential as promising alternatives for managing rice diseases such as blast, brown spot, and sheath blight.

Declaration of Competing Interest

All authors have nothing to declare. None have any conflicts of interest.

Appendix A. Supporting information

Supplementary data associated with this article can be found in the online version at doi:10.1016/j.napere.2026.100188.

Data availability

supplementary material

References

Vieira, N.C., Cortelo, P.C., Castro-Gamboa, I., 2020. Rapid qualitative profiling of metabolites present in *Fusarium solani*, a *rhizospheric fungus* derived from *Senna spectabilis*, using GC/MS and UPLC-QTOF/MSE techniques assisted by UNIFI information system. Eur. J. Mass Spectrom. 26, 281–291.

Mazlan, N.W., et al., 2020. Metabolomics-guided isolation of anti-trypanosomal compounds from endophytic fungi of the mangrove plant *Avicennia lanata*. Curr. Med. Chem. 27, 1815–1835.

Gao, Y.L., et al., 2020. Molecular networking as a dereplication strategy for monitoring metabolites of natural product treated cancer cells. Rapid Commun. Mass Spectrom. 34.

Bushman, T.J., Cunneely, Q., Ciesla, L., 2023. Chapter 3 - Extraction, isolation, and biological activity of natural cyclic dipeptides. Stud. Nat. Prod. Chem. 78, 75–99.

Rao, Q.R., Rao, J.B., Zhao, M., 2023. Chemical diversity and biological activities of specialized metabolites from the genus *Chaetomium*: 2013–2022. Phytochemistry 210.

Tan, B., et al., 2023. Probing the effects of silicon amendment on combined stressors on rice: Lead pollution and blast fungus (*Magnaporthe oryzae*) infection. Ecotoxicol. Environ. Saf. 264.

Hai-Feng, Z., Islam, T., Wen-De, L., 2022. Integrated pest management programme for cereal blast fungus Magnaporthe oryzae. J. Integr. Agric. v. 21, 3420–3433.

Prabhukarthikeyan, S.R., et al., 2019. Bio-protection of brown spot disease of rice and insight into the molecular basis of interaction between Oryza sativa, Bipolaris oryzae and Bacillus amyloliquefaciens. Biol. Control v. 137.

Latif, M., et al., 2022. Interaction among sheath diseases complex of rice and ribosomal DNA analysis for the differentiation of Rhizoctonia solani, R. oryzae and R. oryzae-sativae. Plant Stress v. 5.

Thuy, B.T.P., et al., 2021. A molecular docking simulation study on potent inhibitors against Rhizoctonia solani and Magnaporthe oryzae in rice: silver-tetrylene and bis-silver-tetrylene complexes vs. validamycin and tricyclazole pesticides. Struct. Chem. v. 32, 135–148.

Silva, E.G., et al., 2023. Process intensification of continuous xylitol production in a 3D printing fixedbed microbioreactor by immobilized co-culture of *Saccharomyces cerevisiae* and *Pachysolen tannophilus*. Chem. Eng. Process. - Process. Intensif. 192, 109522.

Pluskal, T., et al., 2010. *MZmine* 2: modular framework for processing, visualizing, and analyzing mass spectrometry-based molecular profile data. BMC Bioinforma. 11, 395.

Dennis, C., Webster, J., 1971. Antagonistic properties of species-groups of *Trichoderma*: II. Production of volatile antibiotics. Trans. Br. Mycol. Soc. 57, 41–IN4.

Zin, N.M., et al., 2020. Profiling of gene expression in methicillin-resistant *Staphylococcus aureus* in response to cyclo-(*L*-Val-*L*-Pro) and chloramphenicol isolated from *Streptomyces sp*., SUK 25 reveals gene downregulation in multiple biological targets. Arch. Microbiol. 202, 2083–2092.

Jamal, Q., et al., 2017. Purification and antifungal characterization of cyclo(*D*-Pro-*L*-Val) from *Bacillus amyloliquefaciens* Y1 against *Fusarium graminearum* to control head blight in wheat. Biocatal. Agric. Biotechnol. 10, 141–147.

Hwang, S.H., et al., 2022. Efficiency and mechanisms of action of pelletized compost loaded with *Bacillus velezensis* CE 100 for controlling tomato Fusarium wilt. Biol. Control 176.

Zheng, X., et al., 2022. Characterization of antifungal cyclic dipeptides of *Lacticaseibacillus paracasei* ZX1231 and active packaging film prepared with its cell-free supernatant and bacterial nanocellulose. Food Res. Int. 162.

Kumar, S.N., Mohandas, C., Nambisan, B., 2013. Purification of an antifungal compound, cyclo(*L*-Pro-*D*-Leu) for cereals produced by *Bacillus cereus subsp*. thuringiensis associated with entomopathogenic nematode. Microbiol. Res. 168, 278–288.

Sibanda, T., et al., 2017. Potential biotechnological capabilities of cultivable mycobiota from carwash effluents. Microbiol. Open 6.

Maluleke, E., et al., 2022. Antifungal activity of non-conventional yeasts against *Botrytis cinerea* and non-*Botrytis* grape bunch rot fungi. Front. Microbiol 13.

Noh, S.W., et al., 2017. Cyclic dipeptides from *Bacillus vallismortis* BS07 require key components of plant immunity to induce disease resistance in arabidopsis against *Pseudomonas* infection. Plant Pathol. J. 33, 402–409.

Wang, X., et al., 2017. Structural diversity and biological activities of the cyclodipeptides from fungi. Molecules 22, 2026.

Tamreihao, K., et al., 2016. *Acidotolerant Streptomyces sp*. MBRL 10 from limestone quarry site showing antagonism against fungal pathogens and growth promotion in rice plants. J. King Saud. Univ. Sci. 30, 143–152.

Xiao, Y., et al., 2023. The RasGEF MoCdc25 regulates vegetative growth, conidiation and appressorium-mediated infection in the rice blast fungus *Magnaporthe oryzae*. Fungal Genet. Biol. 168.

Sena, A.P.A., et al., 2013. Increased enzymatic activity in rice leaf blast suppression by crude extract of *Epicoccum sp*. Trop. Plant Pathol. 38.

Elias, M.T.A., et al., 2023. Molecular networking as a tool to annotate the metabolites of *Bacillus sp*. and *Serratia marcescens* isolates and evaluate their fungistático l effects against *Magnaporthe oryzae* and *Bipolaris oryzae*. 3 Biotech 13, 148.

Klaram, K., Jantasorn, A., Dethoup, T., 2022. Efficacy of marine antagonist, *Trichoderma spp*. as halo-tolerant biofungicide in controlling rice diseases and yield improvement. Biol. Control 172.